Characterization of the glucagon-like peptide-1 receptor in male mouse brain using a novel antibody and in situ hybridization

Jensen, Casper Bo; Pyke, Charles; Rasch, Morten Grønbech; Dahl, Anders Bjorholm; Knudsen, Lotte Bjerre; Secher, Anna

Published in:
Journal of Clinical Endocrinology and Metabolism

Link to article, DOI:
10.1210/en.2017-00812

Publication date:
2017

Document Version
Peer reviewed version

Characterization of the glucagon-like peptide-1 receptor in male mouse brain using a novel antibody and *in situ* hybridization

Casper Bo Jensen, Charles Pyke, Morten Grønbech Rasch, Anders Bjorholm Dahl, Lotte Bjerre Knudsen, Anna Secher

Endocrinology
Endocrine Society

Submitted: September 04, 2017
Accepted: October 23, 2017
First Online: October 30, 2017

Endocrinology; Copyright 2017 DOI: 10.1210/en.2017-00812

Characterization of the glucagon-like peptide-1 receptor in male mouse brain using a novel antibody and *in situ* hybridization

Casper Bo Jensen[1,2], Charles Pyke[1], Morten Grønbech Rasch[1], Anders Bjorholm Dahl[2], Lotte Bjerre Knudsen[1], Anna Secher[1]

[1]*Global Research, Novo Nordisk A/S, Maaloev, Denmark;*

[2]*Image Analysis & Computer Graphics, Department of Applied Mathematics and Computer Science , Technical University of Denmark, Kgs. Lyngby, Denmark;*

Received 04 September 2017. Accepted 23 October 2017.

Glucagon-like peptide-1 (GLP-1) is a physiological regulator of appetite and long-acting GLP-1 receptor agonists (GLP-1RA) lower food intake and bodyweight in both human and animal studies. The effects are mediated through brain GLP-1Rs, and several brain nuclei expressing the GLP-1R may be involved. To date, mapping the complete location of GLP-1R protein in the brain has been challenged by lack of good antibodies and the discrepancy between mRNA and protein especially relevant in neuronal axonal processes. Here, we present a novel and specific monoclonal GLP-1R antibody for immunohistochemistry with murine tissue and show detailed distribution of GLP-1R expression as well as mapping of GLP-1R mRNA by non-radioactive *in situ* hybridization. Semi-automated image analysis was performed to map the GLP-1R distribution to atlas plates from the Allen Institute of Brain Science (AIBS). The GLP-1R was abundantly expressed in numerous regions including the septal nucleus, the hypothalamus and the brain stem. GLP-1R protein expression was also observed on neuronal projections in brain regions devoid of any mRNA which has not been observed in earlier reports. Taken together, these findings provide new knowledge on GLP-1R expression in neuronal cell bodies and neuronal projections.

GLP-1 is a neurotransmitter produced in the brain stem, and an incretin hormone released from gut endocrine L-cells. GLP-1 was shown to have a role in central regulating of feeding in rats and in humans GLP-1 activated brain areas known to regulate food intake. (1). GLP-1 also has an important role in regulating insulin release through activation of the GLP-1R expressed on pancreatic beta cells thereby lowering blood glucose levels (2). The GLP-1R is a G_s protein–coupled receptor (GPCR) (3), and mRNA coding for the receptor is widely expressed in both rodents (4) and humans (5). Longer acting GLP-1RAs lower overall appetite (6) and bodyweight (7) through mechanisms in the brain (8, 9). In rodent models, GLP-1RAs also affect other central functions such as neuroprotection, learning and memory and has been shown to relieve symptoms in Alzheimer and Parkinson's disease models (10). A complete characterization of the localization of GLP-1Rs throughout the brain will aid to delineate GLP-1R signaling in the brain potentially involved in these functions. Although extensive mapping of the receptor mRNA has previously been conducted (11), the mapping of GLP-1R protein distribution by immunohistochemistry (IHC) has been challenged by the lack of specific GLP-1R antibodies (12). Recently, the GLP-1R distribution in the brain was characterized by use of GLP-1R reporter mice (13). Albeit extensive, potential overestimation was emphasized due to the nature of the transgene being expressed at any time in development. Using the primate specific GLP-1R monoclonal antibody (MAb 3F52) (14) we have previously described the GLP-1R distribution in the non-human primate brain (15). Here, we present an additional specific monoclonal GLP-1R antibody (MAb 7F38A2) for the use with murine tissue and show the detailed distribution of

GLP-1R immunoreactivity in combination with a mapping of GLP-1R mRNA by non-radioactive *in situ* hybridization (ISH). Both antibodies have been made available through the Developmental Studies Hybridoma Bank (Department of Biology, University of Iowa, Iowa City, IA).The GLP-1R distribution was mapped by image segmentation following semi-automatic registration of the scanned histological slides to digital atlas plates from the AIBS mouse brain reference model (16, 17). IHC was performed on brain tissue derived from mice with a complete knock out of the GLP-1R (*Glp-1r*$^{-/-}$) to further validate the antibody.

Materials and Methods:

Generation of anti-mouse GLP-1 receptor antibody

GLP-1R monoclonal antibody (7F38A2 3,6mg/ml) was generated at Novo Nordisk A/S. *Glp-1r*$^{-/-}$ mice were immunized with baby hamster kidney (BHK) cells stably transfected with the mouse GLP-1R and antibodies were generated using standard hybridoma technology. The *Glp-1r*$^{-/-}$ mice were on a C57BL background and were derived from the previously described *Glp-1r*$^{-/-}$ strain (18) custom bred by Novo Nordisk A/S at Taconic. The strain is not commercially available. GLP-1R specific antibodies were identified by image based screening (ImageXpress, Molecular Devices, CA) using the BHK-mouse GLP-1R (mGLP-1R) cells used for immunization and a mock transfected BHK cell-line for counter screen. Following isolation of the 7F38A2 clone and purification of the antibody, binding to mGLP-1R was validated in a flow cytometry experiment using transiently transfected HEK-mGLP-1R and HEK mock cells. Detection was done using an allophycocyanin-labelled anti-mouse antibody (#115-136-071, Jackson Immunoresearch, PA) diluted 1:500. The 7F38A2 antibody is a mouse IgG2aκ and anti-TNP is an isotype control. For the immunostaining experiments the antibody was biotinylated using NHS-biotin (#H1759, Sigma) following the manufacturer's instructions.

The antibody is now available at http://dshb.biology.uiowa.edu/Mab-7F38?sc=9&category=-109

Animals

Male mice (C57BL/6J, and *Glp1r*$^{-/-}$) and rats (Sprague Dawley) were obtained from Taconic, Denmark and housed 5 per cage in standard, temperature controlled conditions with a 12-hour light/dark cycle. The animals had ad libitum access to water and regular chow (no. 1324, Altromin, Brogaarden) unless otherwise stated. Handling and housing of the animals were conducted in accordance with approved national regulations in Denmark which are fully compliant with internationally accepted principles for the care and use of laboratory animals, and with animal experimental licenses granted by the Danish Ministry of Justice.

Tissue preparation and sectioning

The animals were anesthetized with isoflurane and transcardially perfused with heparinized (10U/ml) saline (10 ml) followed by 10 % neutral buffered formalin (NBF) (10 ml). Brains were removed, immersed into 10 % NBF and stored at room temperature for 24 hours before being embedded into paraffin. For whole brain receptor mapping one male mouse was used, and the entire brain was sectioned at 4.5 µm intervals and all sections were collected. Additionally, two male mice (one C57BL/6J, one *Glp-1r-/-*) and one male rat (Sprague Dawley) were used for a follow up study. Section thickness was 4.5 µm.

Immunohistochemistry

For whole brain receptor mapping every 20th section was used for IHC. Paraffin sections were dewaxed and rehydrated in double distilled water. Sections were treated with 0.1 % pronase in

PBS at 37°C for 10 minutes and rinsed in Tris-buffered saline (TBS). Sections were then treated with 1 % H_2O_2 in TBS for 15 minutes, washed in TBS with 0.05 % Tween (TBS-T), blocked with avidin for 10 minutes (Dako, Glostrup, Denmark), washed with TBS-T, blocked with biotin for 10 minutes (Dako, Glostrup, Denmark), washed with TBS-T, and pre-incubated with 3.2 mg/mL Poly L-Lysine, 3 % BSA bovine serum albumin, 7 % donkey serum and 3 % skimmed milk (Dako, Glostrup, Denmark) for 30 minutes. Sections were incubated overnight with primary biotinylated mouse GLP-1R antibody (MAb 7F38A2, Novo Nordisk, Måløv, Denmark) then washed three times for 10 minutes each in TBS-T, followed by treatment with Vectastain ABComplexHRP in TBS for 30 minutes and washed again three times for 10 minutes each. Sections were developed with diaminobenzidine **(**DAB^+) (Dako, Glostrup, Denmark) and counterstained with hematoxylin, rinsed in water, dehydrated and mounted. Sections for the follow up study were stained with similar protocol with the exception of an additional Tyramide Signal Amplification (TSA) step and treatment with Vectastain ABComplexHRP, following primary antibody incubation which this time was reduced to two hours. All images were obtained using Hamamatsu NanoZoomer-XR. In addition, the staining protocol has been optimized for automatic staining applying the Ventana Discovery Ultra staining module. For details on this protocol please refer to the supplementary material.

In situ hybridization

ISH was performed using the RNAscope platform (19, 20) on neighboring sections to the sections used for whole brain IHC mapping. The staining was performed using a Ventana Discovery XT system (Ventana MedicalSystems, Inc., Tucson, AZ) with RNAscope VS FFPE RED reagent kit (cat# 320610 from Advanced Cell Diagnostics, Hayward, CA). Briefly, the VS RNAscope protocol was used with the following pretreatment conditions: boiling for 2 minutes and pretreatment 2+3 steps for 4 minutes each with probes for bacterial DapB (negative control, cat. no. 310048), and mouse GLP-1R (cat. no. 415896). Images were obtained using Hamamatsu NanoZoomer-XR.

To validate the signal obtained for GLP-1R mRNA, another mouse GLP-1R probe (no. 415906) non-overlapping in sequence with probe no. 415896 was used on adjacent sagittal mouse brain sections. The signals obtained with both probes showed a complete overlap (data not shown).

Image analysis and atlas plate generation

Image segmentation of the IHC and ISH slide scanner images were performed using a multinomial regression classifier trained on a constructed mosaic image for each staining type. The r,g,b values of the images were used as input features. Prior to segmentation each IHC/ISH image pair was registered to a digital atlas plate obtained from the AIBS mouse brain reference model (16, 17). The specific atlas plates were manually selected from a collection of 528 plates. The image registration was performed in a coarse to fine manner with an affine transformation followed by non-linear b-spline transformation using sum of squared difference as similarity measure. All registrations were computed using Elastix (21). The final atlas plates were constructed by summing segmented signal inside a square mask moving across the registered images. A blue circle (IHC) or a red square (ISH) was drawn on the atlas plate if positive signal was detected. The diameter of the marker was based on the signal count applying a logarithmic scale to show both weak and strong signals. Following the automatic atlas plate generation manual corrections were performed in regions where the automatic image registration was not sufficiently accurate.

Results

Antibody specificity

IHC staining with the GLP-1R antibody revealed high intensity staining with good resolution and low background (Figure 1). The antibody was specific for GLP-1Rs expressed in peripheral organs such as the Brunner's gland (Figure 1, A-B) and further for mouse (Figure 1, C-F) and rat (Figure 1, G-H) brain. The expressional profile of GLP-1R was evaluated throughout the entire mouse brain, and this expression was confirmed in select regions in the rat brain in hypothalamus and brain stem showing correspondence between the two species in the regions investigated. However, some discrepancies existed between mouse and rat where GLP-1R expression could be observed in mouse lateral habenula, nucleus accumbens and in the nucleus of the lateral olfactory tract/cortical amygdalar area which was absent in rat brain (data not shown). Validation of the antibody has further been performed for GLP-1Rs in pancreas (22), kidney (23) and other peripheral GLP-1R expressing organs such as GI tract, lung and thyroid (data not shown).

Distribution of GLP-1R

Overall, GLP-1R protein and mRNA co-localized in most regions, however, some discrepancies was found such as in the posterior hippocampus, median eminence and terminal field of accessory olfactory bulb projections. The findings are summarized in Table 2 and on the atlas plate overlays (Figure 2, Figure 3).

Telencephalon.

In agreement with previous reports, GLP-1R protein positive cells were identified in the olfactory bulb, amygdala, dentate gyrus, septal nucleus, preoptic area, septofimbrial nucleus, triangular nucleus of septum, tenia tecta, vascular organ of the laminae terminalis, nucleus accumbens and bed nucleus of stria terminalis. Furthermore, protein was observed in the subfornical organ and in the terminal field of accessory olfactory bulb projections (the latter is included in the cortical amygdalar area in Table 2) where mRNA expression was absent (Table 2). Especially in those regions where protein expression differed from mRNA expression, the specificity of the antibody was further validated by antibody staining on brain sections from *Glp-1r* $^{-/-}$ mice. The data from the *Glp-1r*$^{-/-}$ mice showed complete absence of GLP-1R immunoreactivity, further establishing this antibody as specific towards the GLP-1R and confirming the presence of GLP-1R protein in these regions (Figure 4).

Diencephalon.

In the diencephalon GLP-1R protein and mRNA was observed in cells in zona incerta, tuberal nucleus, peripeduncular nucleus, and in hypothalamus in the arcuate nucleus, dorsomedial hypothalamic nucleus, lateral hypothalamic nucleus, paraventricular hypothalamic nucleus and supraoptic nucleus. Furthermore, GLP-1R protein was observed in median eminence as fibers only with no mRNA expression. The same pattern of presence of GLP-1R protein in the absence of mRNA expression was observed in the geniculate group of thalamus, posterior hypothalamic nucleus, habenula, and retrochiasmatic area (Table 2). When comparing mRNA expression reported by AIBS (http://www.brain-map.org/) with data obtained in the present study several areas expressing GLP-1R mRNA in the AIBS atlas were negative in the present study (Table 2).

Mesencephalon.

GLP-1R was observed in the anterior pretectal nucleus, medial and posterior pretectal area, the periaqueductal gray, and in the substantia nigra. GLP-1R protein was also observed in the motor related part of superior colliculus whereas mRNA expression could be observed in both the

motor related and the sensory related part of superior colliculus. Further discrepancies were observed in the dorsal raphe, the medial mammillary nucleus, the midbrain reticular nucleus and the ventral spinocerebellar tract where receptor was observed as protein on fibers only, lacking mRNA expression.

Pons.
In pons, GLP-1R protein and mRNA expression could be observed in the pontine grey, the parabrachial nucleus and the principal sensory nucleus of the trigeminal. Very few brain regions were positive for both protein and mRNA and only protein was observed in the nucleus incertus, nucleus of the lateral lemniscus, and the superior olivary complex whereas only mRNA was observed in the pontine reticular nucleus.

Medulla.
In Medulla, GLP-1R was observed in the area postrema, cuneate nucleus, inferior olivary complex, lateral reticular nucleus, nucleus tractus solitarus, medial vestibular nucleus, and the spinal nucleus of the trigeminal. GLP-1R protein but not mRNA was observed in the dorsal motor nucleus of the vagus nerve and in flocculus, residing in cerebellum, whereas mRNA was evident in nucleus ambiguus, and in the reticular nucleus.

Discussion

The reliable detection of the GLP-1R expression in tissues using IHC has been hampered by a lack of specific antibodies thus limiting well validated histological mapping studies to the detection of GLP-1R mRNA using ISH (12, 24, 25) and protein using *in situ* ligand binding with low spatial resolution (26). In this study an extensive mapping of GLP-1R mRNA and protein expression in the mouse brain is reported. For localization of GLP-1R protein a monoclonal GLP-1R antibody was used which is highly specific for murine GLP-1R as demonstrated by the complete absence of reactivity in mice lacking the GLP-1R. The localization of GLP-1R protein was combined with detection of GLP-1R mRNA on adjacent sections using non-radioactive ISH, enabling a higher accuracy for anatomical localization compared to a radioactivity based approach. The expression patterns observed showed good alignment between protein and mRNA expression but also revealed some regions only positive for GLP-1R protein and encompassing axonal projections. This is a well described phenomenon in the brain where protein and gene expression do not always correlate (27, 28, 29), possibly in situations where protein can be transported away from the nuclear processing site along the axonal processes. This phenomenon necessitates caution when interpreting potential GLP-1 interacting brain regions and neurons based on receptor mRNA expression alone, as such data will underestimate the number of GLP-1 binding sites. The distribution of GLP-1R protein in the mouse brain has previously been described using a transgene *Glp-1r* reporter mouse (13). When comparing GLP-1R protein expression detected using the antibody in the present study with the study by Cork et al (13) there is a high level of agreement with a few exceptions where some positive regions were seen using IHC but not reported by Cork et al. Of note, several of these regions were regions lacking mRNA expression, indicating the presence of protein exclusively on projections and terminals. Thus, IHC seems an easier approach to obtain high sensitivity for GLP-1R expression including axonal processes, without requiring generation of reporter mice. Interestingly, the concern for artefactual overexpression of GLP-1R in the *Glp-1r* reporter mouse as a result of accumulated gene transcription during embryogenesis does not seem to be a problem in the case of the GLP-1R, as all regions reported positive in the reporter mouse were also seen with antibody staining.

Comparing mRNA expression in the present study to that reported by AIBS revealed several areas where mRNA was reported to be present by AIBS (e.g. nucleus of the trapezoid body, septohippocampal nucleus, dorsal peduncular area, and tegmental reticular nucleus) but not observed in our study (and hence not included in Table 2). These inconsistencies are likely due to a higher specificity of the RNAscope ISH platform used here as demonstrated by the full overlap of signals obtained with two non-overlapping probes for GLP-1R. Another explanation could be the more extensive sampling of the mouse brain in studies reported by AIBS potentially revealing sub nuclei with limited GLP-1R expression that was not picked up in this study.

To verify that the antibody could also be applied to rat tissue, select sections from rat brain were stained and examined. Although there was a good agreement with respect to localization of the GLP-1R between mouse and rat on sections with hypothalamus and brain stem, it must be emphasized that the entire rat brain was not analyzed and a discrepancy between mouse and rat in GLP-1R localization in the brain was detected in some regions. In general more GLP-1R protein was observed in the mouse brain compared to the rat brain. A large part of the additional GLP-1R protein was seen in mouse axonal processes such as in medial habenula and cortical amygdalar area which were absent in the rat. Thus, to fully characterize the GLP-1R in rat brain a full mapping is needed rather than assuming complete correspondence between species.

Considering the relative small fraction of neurons in the hindbrain that produce GLP-1, a remarkable abundance of GLP-1Rs were found to be expressed throughout the brain indicating potential diverse actions of this neurotransmitter. Indeed, central GLP-1 activity has been reported to affect functions such as feeding behavior, body weight and temperature, malaise, fluid homeostasis, stress response, and learning and memory (30, 31). One of the most abundant GLP-1R populations was found in the caudal division of the lateral septal nucleus a population that is little understood with respect to GLP-1 actions. The caudal part of lateral septal nucleus has been characterized as abundant in somatostatin neurons which has been shown to act inhibitory in septal nucleus (32, 33). Further building on this inhibitory mechanism, other studies have suggested that GLP-1R expressing neurons in LS are GABA'ergic and connected to GLP-1 actions on behaviors associated with reward (34, 35). Septal projections are extensive and include innervation of hypothalamus, supramammilary nucleus, hippocampus, thalamus, and ventral tegmental area (36). Thus the involvement in reward signaling may only be a one GLP-1 mediated behavior initialized from this area.

Another area with high expression of GLP-1R positive fibers was in the dentate gyrus which is the principal input to the rest of the hippocampus forming the "tri-synaptic hippocampal circuit" associated with episodic memory consolidation and formation (37). The dentate gyrus is capable of generating new granule cells in the adult brain (38, 39), which has been linked to memory formation and maintenance as well as neuroprotection (40, 41). Hence, GLP-1R expression in this area could be coupled to some of the beneficial effects reported with GLP-1 regulation of memory and Alzheimer's disease (42) and neuroprotection (31).

A high expression of GLP-1R was also identified on fibers projecting to the median eminence. The median eminence is usually associated with the integration of the hypothalamic pituitary axis serving as an area of release from paraventricular hypothalamic neurons to the bloodstream. On top of this, literature suggests the median eminence to be a site for uptake of peripheral peptides such as leptin and ghrelin from the blood (43, 44) through receptor specific uptake; this could be extended to include GLP-1RAs. Indeed all circumventricular organs including the median eminence have a high expression of GLP-1R suggesting interaction with peripheral GLP-1 in these regions.

In summary, we report here a full mapping of GLP-1R protein and mRNA in the mouse brain using IHC with a specific monoclonal antibody and ISH, respectively. The strength of using a fully validated and specific antibody is emphasized by the ability to detect GLP-1R protein in regions devoid of mRNA and in neuronal projections where it was not observed using a transgenic reporter system.

Acknowledgements
The technical assistance of Pia G. Mortensen, Bettina Brandrup and Suzanne K. Møller is gratefully acknowledged.

Address all correspondence and requests for reprints to: Lotte Bjerre Knudsen, Novo Nordisk, Novo Nordisk Park, DK-2760 Maaloev, Denmark. E-mail: lbkn@novonordisk.com.

Disclosure Summary: C.J, C.P, M.G, L.B.K and A.S are employed by Novo Nordisk A/S, which markets the GLP-1RA liraglutide for the treatment of diabetes and weight management, and hold minor stock portions as part of an employee offering program. A.B.D has nothing to declare.

References

1. Turton M, O'Shea D, Gunn I et al. A role for glucagon-like peptide-1 in the central regulation of feeding. *Nature*. 1996;379(6560):69-72. doi:10.1038/379069a0.
2. Zander M, Madsbad S, Madsen J, Holst J. Effect of 6-week course of glucagon-like peptide 1 on glycaemic control, insulin sensitivity, and β-cell function in type 2 diabetes: a parallel-group study. *The Lancet*. 2002;359(9309):824-830. doi:10.1016/s0140-6736(02)07952-7.
3. Brubaker P, Drucker D. Structure-Function of the Glucagon Receptor Family of G Protein-Coupled Receptors: The Glucagon, GIP, GLP-1, and GLP-2 Receptors. *Receptors and Channels*. 2002;8:179-188. doi:10.1080/10606820213687.
4. Campos R. Divergent tissue-specific and developmental expression of receptors for glucagon and glucagon-like peptide-1 in the mouse. *Endocrinology*. 1994;134(5):2156-2164. doi:10.1210/en.134.5.2156.
5. Wei Y, Mojsov S. Tissue-specific expression of the human receptor for glucagon-like peptide-I: brain, heart and pancreatic forms have the same deduced amino acid sequences. *FEBS Letters*. 1995;358(3):219-224. doi:10.1016/0014-5793(94)01430-9.
6. van Can J, Sloth B, Jensen C, Flint A, Blaak E, Saris W. Effects of the once-daily GLP-1 analog liraglutide on gastric emptying, glycemic parameters, appetite and energy metabolism in obese, non-diabetic adults. *International Journal of Obesity*. 2013;38(6):784-793. doi:10.1038/ijo.2013.162.
7. O'Neil P, Garvey W, Gonzalez-Campoy J et al. EFFECTS OF LIRAGLUTIDE 3.0 MG ON WEIGHT AND RISK FACTORS IN HISPANIC VERSUS NON-HIPANIC POPULATIONS: SUBGROUP ANALYSIS FROM SCALE RANDOMIZED TRIALS. *Endocrine Practice*. 2016;22(11):1277-1287. doi:10.4158/ep151181.or.
8. Secher A, Jelsing J, Baquero A et al. The arcuate nucleus mediates GLP-1 receptor agonist liraglutide-dependent weight loss. *Journal of Clinical Investigation*. 2014;124(10):4473-4488. doi:10.1172/jci75276.
9. Sisley S, Gutierrez-Aguilar R, Scott M, D'Alessio D, Sandoval D, Seeley R. Neuronal GLP1R mediates liraglutide's anorectic but not glucose-lowering effect. *Journal of Clinical Investigation*. 2014;124(6):2456-2463. doi:10.1172/jci72434.

10. McClean P, Parthsarathy V, Faivre E, Holscher C. The Diabetes Drug Liraglutide Prevents Degenerative Processes in a Mouse Model of Alzheimer's Disease. *Journal of Neuroscience*. 2011;31(17):6587-6594. doi:10.1523/jneurosci.0529-11.2011.
11. Merchenthaler I, Lane M, Shughrue P. Distribution of pre-pro-glucagon and glucagon-like peptide-1 receptor messenger RNAs in the rat central nervous system. *The Journal of Comparative Neurology*. 1999;403(2):261-280. doi:10.1002/(sici)1096-9861(19990111)403:2<261::aid-cne8>3.0.co;2-5.
12. Pyke C, Knudsen L. The Glucagon-Like Peptide-1 Receptor—or Not?. *Endocrinology*. 2013;154(1):4-8. doi:10.1210/en.2012-2124.
13. Cork S, Richards J, Holt M, Gribble F, Reimann F, Trapp S. Distribution and characterisation of Glucagon-like peptide-1 receptor expressing cells in the mouse brain. *Molecular Metabolism*. 2015;4(10):718-731. doi:10.1016/j.molmet.2015.07.008.
14. Pyke C, Heller R, Kirk R et al. GLP-1 Receptor Localization in Monkey and Human Tissue: Novel Distribution Revealed With Extensively Validated Monoclonal Antibody. *Endocrinology*. 2014;155(4):1280-1290. doi:10.1210/en.2013-1934.
15. Heppner K, Kirigiti M, Secher A et al. Expression and Distribution of Glucagon-Like Peptide-1 Receptor mRNA, Protein and Binding in the Male Nonhuman Primate (Macaca mulatta) Brain. *Endocrinology*. 2015;156(1):255-267. doi:10.1210/en.2014-1675.
16. Oh S, Harris J, Ng L et al. A mesoscale connectome of the mouse brain. *Nature*. 2014;508(7495):207-214. doi:10.1038/nature13186.
17. Lein E.S, Hawrylycz M.J, Ao N et al. Genome-wide atlas of gene expression in the adult mouse brain. *Nature*, 2007;445(7124):168-176. doi:10.1038/nature05453.
18. Scrocchi L, Brown T, Maclusky N et al. Glucose intolerance but normal satiety in mice with a null mutation in the glucagon–like peptide 1 receptor gene. *Nature Medicine*. 1996;2(11):1254-1258. doi:10.1038/nm1196-1254.
19. Wang F, Flanagan J, Su N et al. RNAscope: a novel in situ RNA analysis platform for formalin-fixed, paraffin-embedded tissues. *The Journal of Molecular Diagnostics*. 2012;14(1):22-29. doi:10.1016/j.jmoldx.2011.08.002.
20. Anderson C, Zhang B, Miller M et al. Fully Automated RNAscope In Situ Hybridization Assays for Formalin-Fixed Paraffin-Embedded Cells and Tissues. *Journal of Cellular Biochemistry*. 2016;117(10):2201-2208. doi:10.1002/jcb.25606.
21. Klein S, Staring M, Murphy K, Viergever, M. A, Pluim J.P. Elastix: a toolbox for intensity-based medical image registration. *IEEE transactions on medical imaging*. 2010;29(1):196-205. doi:10.1109/TMI.2009.2035616.
22. Lehtonen J, Schäffer L, Rasch M, Hecksher-Sørensen J, Ahnfelt-Rønne J. Beta cell specific probing with fluorescent exendin-4 is progressively reduced in type 2 diabetic mouse models. *Islets*. 2015;7(6):e1137415. doi:10.1080/19382014.2015.1137415.
23. Jensen E, Poulsen S, Kissow H et al. Activation of GLP-1 receptors on vascular smooth muscle cells reduces the autoregulatory response in afferent arterioles and increases renal blood flow. *American Journal of Physiology - Renal Physiology*. 2015;308(8):F867-F877. doi:10.1152/ajprenal.00527.2014.
24. Panjwani N, Mulvihill E, Longuet C et al. GLP-1 Receptor Activation Indirectly Reduces Hepatic Lipid Accumulation But Does Not Attenuate Development of Atherosclerosis in Diabetic MaleApoE−/−Mice. *Endocrinology*. 2013;154(1):127-139. doi:10.1210/en.2012-1937.
25. Drucker D. Never Waste a Good Crisis: Confronting Reproducibility in Translational Research. *Cell Metabolism*. 2016;24(3):348-360. doi:10.1016/j.cmet.2016.08.006.

26. Göke R, Larsen P, Mikkelsen J, Sheikh S. Distribution of GLP-1 Binding Sites in the Rat Brain: Evidence that Exendin-4 is a Ligand of Brain GLP-1 Binding Sites. *European Journal of Neuroscience*. 1995;7(11):2294-2300. doi:10.1111/j.1460-9568.1995.tb00650.x.
27. Komorowski A, James G.M, Philippe C et al. Association of Protein Distribution and Gene Expression Revealed by PET and Post-Mortem Quantification in the Serotonergic System of the Human Brain. *Cerebral Cortex*. 2017;27(1):117-130. doi:10.1093/cercor/bhw355.
28. Fortelny N, Overall C, Pavlidis P, Freue G. Can we predict protein from mRNA levels?. *Nature*. 2017;547(7664):E19-E20. doi:10.1038/nature22293.
29. Liu Y, Beyer A, Aebersold R. On the Dependency of Cellular Protein Levels on mRNA Abundance. *Cell*. 2016;165(3):535-550. doi:10.1016/j.cell.2016.03.014.
30. Vrang N, Larsen P. Preproglucagon derived peptides GLP-1, GLP-2 and oxyntomodulin in the CNS: Role of peripherally secreted and centrally produced peptides. *Progress in Neurobiology*. 2010;92(3):442-462. doi:10.1016/j.pneurobio.2010.07.003.
31. During M, Cao L, Zuzga D et al. Glucagon-like peptide-1 receptor is involved in learning and neuroprotection. *Nature Medicine*. 2003;9(9):1173-1179. doi:10.1038/nm919.
32. Risold P, Swanson L. Chemoarchitecture of the rat lateral septal. *Brain Research Reviews*. 1997;24(2-3):91-113. doi:10.1016/s0165-0173(97)00008-8.
33. Twery M, Gallagher J. Somatostatin hyperpolarizes neurons and inhibits spontaneous activity in the rat dorsolateral septal nucleus. *Brain Research*. 1989;497(2):315-324. doi:10.1016/0006-8993(89)90277-1.
34. Harasta A, Power J, von Jonquieres G et al. Septal Glucagon-Like Peptide 1 Receptor Expression Determines Suppression of Cocaine-Induced Behavior. *Neuropsychopharmacology*. 2015;40(8):1969-1978. doi:10.1038/npp.2015.47.
35. Reddy I, Pino J, Weikop P et al. Glucagon-like peptide 1 receptor activation regulates cocaine actions and dopamine homeostasis in the lateral septum by decreasing arachidonic acid levels. *Translational Psychiatry*. 2016;6(5):e809. doi:10.1038/tp.2016.86.
36. Risold P, Swanson L. Connections of the rat lateral septal complex. *Brain Research Reviews*. 1997;24(2-3):115-195. doi:10.1016/s0165-0173(97)00009-x.
37. Amaral D, Witter M. The three-dimensional organization of the hippocampal formation: A review of anatomical data. *Neuroscience*. 1989;31(3):571-591. doi:10.1016/0306-4522(89)90424-7.
38. Ming G, Song H. ADULT NEUROGENESIS IN THE MAMMALIAN CENTRAL NERVOUS SYSTEM. *Annual Review of Neuroscience*. 2005;28(1):223-250. doi:10.1146/annurev.neuro.28.051804.101459.
39. Cameron H, Mckay R. Adult neurogenesis produces a large pool of new granule cells in the dentate gyrus. *The Journal of Comparative Neurology*. 2001;435(4):406-417. doi:10.1002/cne.1040.
40. Kitamura T, Saitoh Y, Takashima Net al. Adult neurogenesis modulates the hippocampus-dependent period of associative fear memory. *Cell*. 2019;139(4):814-827. doi:10.1016/j.cell.2009.10.020.
41. Madroñal N, Delgado-García J, Fernández-Guizán A et al. Rapid erasure of hippocampal memory following inhibition of dentate gyrus granule cells. *Nature Communications*. 2016;7:10923. doi:10.1038/ncomms10923.
42. McClean P.L, Parthsarathy V, Faivre E, Hölscher C. The diabetes drug liraglutide prevents degenerative processes in a mouse model of Alzheimer's disease. *Journal of Neuroscience*, 2011;31(17):6587-6594. doi:10.1523/JNEUROSCI.0529-11.2011.

43. Schaeffer M, Langlet F, Lafont C et al. Rapid sensing of circulating ghrelin by hypothalamic appetite-modifying neurons. *Proceedings of the National Academy of Sciences*. 2013;110(4):1512-1517. doi:10.1073/pnas.1212137110.
44. Balland E, Dam J, Langlet F et al. Hypothalamic Tanycytes Are an ERK-Gated Conduit for Leptin into the Brain. *Cell Metabolism.* 2014;19(2):293-301. doi:10.1016/j.cmet.2013.12.015.

Figure 1. GLP-1R IHC with antibody Mab 7F38A2 on paraffin-embedded mouse Brunner's Gland (A–B) and mouse brain (C-F). B, High magnification of the solid-line box in A. E and F, Magnifications of solid-line boxed areas in C and D, respectively. C and E are from a *Glp-1r*$^{-/-}$ mouse while D and F are from a C57BL/6J mouse. GLP-1R IHC with antibody Mab 7F38A2 on paraffin-embedded rat brain (G–H). G, High magnification image of the hypothalamus showing positive staining in arcuate hypothalamic nucleus and median eminence. H, High magnification image showing positive staining in area postrema, dorsal motor nucleus of the vagus nerve and nucleus of the solitary tract. Scale bar in A corresponds to 2000 um. Scale bar in B corresponds to 100 um. Scale bar in C-D corresponds to 2000 um. Scale bar in E-F corresponds to 250 um. Scale bar in G corresponds to 500 um. Scale bar in H corresponds to 500 um.

Figure 2. Atlas plates (bregma 2.86 to -1.70) showing distribution of signals for mouse GLP-1R *ISH* (red squares) and GLP-1R IHC (blue circles). The distribution is overlaid onto digital atlas plates constructed from the AIBS mouse brain atlas. The distribution of GLP-1R mRNA and protein are indicated on the left half of the atlas plates and brain regions with positive staining for either GLP-1R mRNA or protein are highlighted with a solid color on the right half of the atlas plates. Brain region abbreviations follow the nomenclature of the AIBS mouse brain reference atlas which can be found at: http://atlas.brain-map.org/

Figure 3. Atlas plates (bregma -3.16 to -7.32) showing distribution of signals for mouse GLP-1R *ISH* (red squares) and GLP-1R IHC (blue circles). The distribution is overlaid onto digital atlas plates constructed from the AIBS mouse brain atlas. The distribution of GLP-1R mRNA and protein are indicated on the left half of the atlas plates and brain regions with positive staining for either GLP-1R mRNA or protein are highlighted with a solid color on the right half of the atlas plates. Brain region abbreviations follow the nomenclature of the AIBS mouse brain reference atlas which can be found at: http://atlas.brain-map.org/

Figure 4. High magnification images of adjacent sections of C57BL/6J mouse brain tissue focusing on terminal field of accessory olfactory bulb projections (A-B). A, Mouse GLP-1R *ISH* showing lack of signal. B, GLP-1R IHC with antibody Mab 7F38A2 showing positive staining. C, GLP-1R IHC with antibody Mab 7F38A2 on a corresponding section from a *Glp1r*$^{-/-}$ mouse brain showing negative staining. Scale bars correspond to 400 um.

Table 1. Antibody Table

Peptide/Protein Target	Name of antibody	Manufacturer, Catalog #, and/or Name of Individual Providing the Antibody	Species Raised in; Monoclonal or Polyclonal	Dilution Used	RRID
GLP-1R	MAb 7F38A2	Developmental Studies Hybridoma Bank, Mab 7F38	Mouse, Monoclonal	1:720	AB_2618101

Table 2. Summary of GLP-1R (IHC and ISH) location in C57BL/6J mouse brain and comparison to external references

Structure	Area		Protein	mRNA	Cork et al (13) (protein)	AIBS (mRNA)
Telencephalon	AOB	Accessory olfactory bulb	+	+	+	+
	BMA	Basomedial amygdalar nucleus	+	-	+	+
	CeA	Central amygdala	+	+	+	+
	CeA/AAA	Central amygdala/Anterior amygdalar area	+	+	+	+
	COA	Cortical amygdalar area	+	-	+	+
	DG	Dentate gurys	+	+	+	+
	LPO	Lateral preoptic area	+	+	+	+
	LS	Lateral septal nucleus	+	+	+	+
	NLOT/COA	Nucleus of the lateral olfactory tract/Cortical amygdalar area	+	-	+	+
	PA	Posterior amygdalar nucleus	+	-	+	+
	SF	Septofimbrial nucleus	+	+	NA	+
	SFO	Subfornical organ	+	+	+	+
	TRS	Triangular nucleus of septum	-	+	NA	+
	TT	Tenia tecta	+	+	+	+
	OV	Vascular organ of the laminae terminalis	+	NA	+	NA
	ACB	Nucleus accumbens	+	+	+	+
	BST	Bed nucleus of stria terminalis	+	+	+	+
Diencephalon	ARH	Arcuate hypothalamic nucleus	+	+	+	+
	DMH	Dorsomedial hypothalamic nucleus	+	+	+	+
	GENd	Geniculate group, dorsal thalamus	+	-	+	+
	Hb	Habenula	+	-	+	+
	LHA	Lateral hypothalamic nucleus	+	+	+	+
	ME	Median eminence	+	-	NA	+
	PH	Posterior hypothalamic nucleus	+	-	+	+
	PP	Peripeduncular nucleus	+	+	NA	+
	PVH	Paraventricular hypothalamic nucleus	+	+	+	+
	RCH	Retrochiasmatic area	+	-	+	+
	SO	Supraoptic nucleus	+	+	NA	+
	TU	Tuberal nucleus	+	+	NA	+
	ZI	Zona incerta	+	+	+	+
Mesencephalon	APN	Anterior pretectal nucleus	+	+	+	+
	DR	Dorsal raphe	+	-	NA	+
	MM	Medial mammillary nucleus	+	-	+	+
	MPT	Medial pretectal area	+	+	+	+
	MRN	Midbrain reticular nucleus	+	-	NA	+
	PAG	Periaqueductal gray	+	+	+	+
	PPT	Posterior pretectal area	+	+	+	+
	SCs	Superior colliculus, sensory related	-	+	NA	+
	SCm	Superior colliculus, motor related	+	+	NA	+
	SCTV	ventral spinocerebellar tract	+	-	NA	+
	SNr	Substantia nigra, reticular part	+	+	NA	+
	SNc	Substantia nigra, compact part	+	+	NA	+
Pons	NI	Nucleus incertus	+	-	NA	+
	NLL	Nucleus of the lateral lemniscus	+	-	NA	+
	PB	Parabrachial nucleus	+	+	NA	+
	PCG	Pontine central gray	+	-	NA	+

	PG	Pontine gray	+	+	NA	+
	PRNc	Pontine reticular nucleus, caudal part	-	+	NA	+
	PRNr	Pontine reticular nucleus	-	+	NA	+
	PSV	Principal sensory nucleus of the trigeminal	+	+	NA	+
	SOC	Superior olivary complex	+	-	NA	+
Medulla	AMB	Nucleus ambiguus	-	+	NA	+
	AP	Area postrema	+	+	+	+
	CU	Cuneate nucleus	+	+	NA	+
	DMX	Dorsal motor nucleus of the vagus nerve	+	-	NA	+
	ECU	External cuneate nucleus	+	+	NA	+
	FL	Flocculus (cerebellum)	+	-	NA	+
	IO	Inferior olivary complex	+	+	+	+
	LRNm	Lateral reticular nucleus, magnocellular part	+	+	NA	+
	MARN	Magnocellular reticular nucleus	-	+	NA	+
	MDRN	Medullary reticular nucleus	-	+	NA	+
	MV	Medial vestibular nucleus	+	+	NA	+
	NTS	Nucleus tractus solitarus	+	+	+	+
	PARN	Parvicellular reticular nucleus	-	+	NA	+
	SPVC	Spinal nucleus of the trigeminal, caudal part	+	+	NA	+

Presence (+) or absence (-) of GLP-1R protein and mRNA in mouse brain. The two right columns indicate whether GLP-1R was observed as protein (Cork et al) or mRNA (AIBS). NA: not assessed/reported.

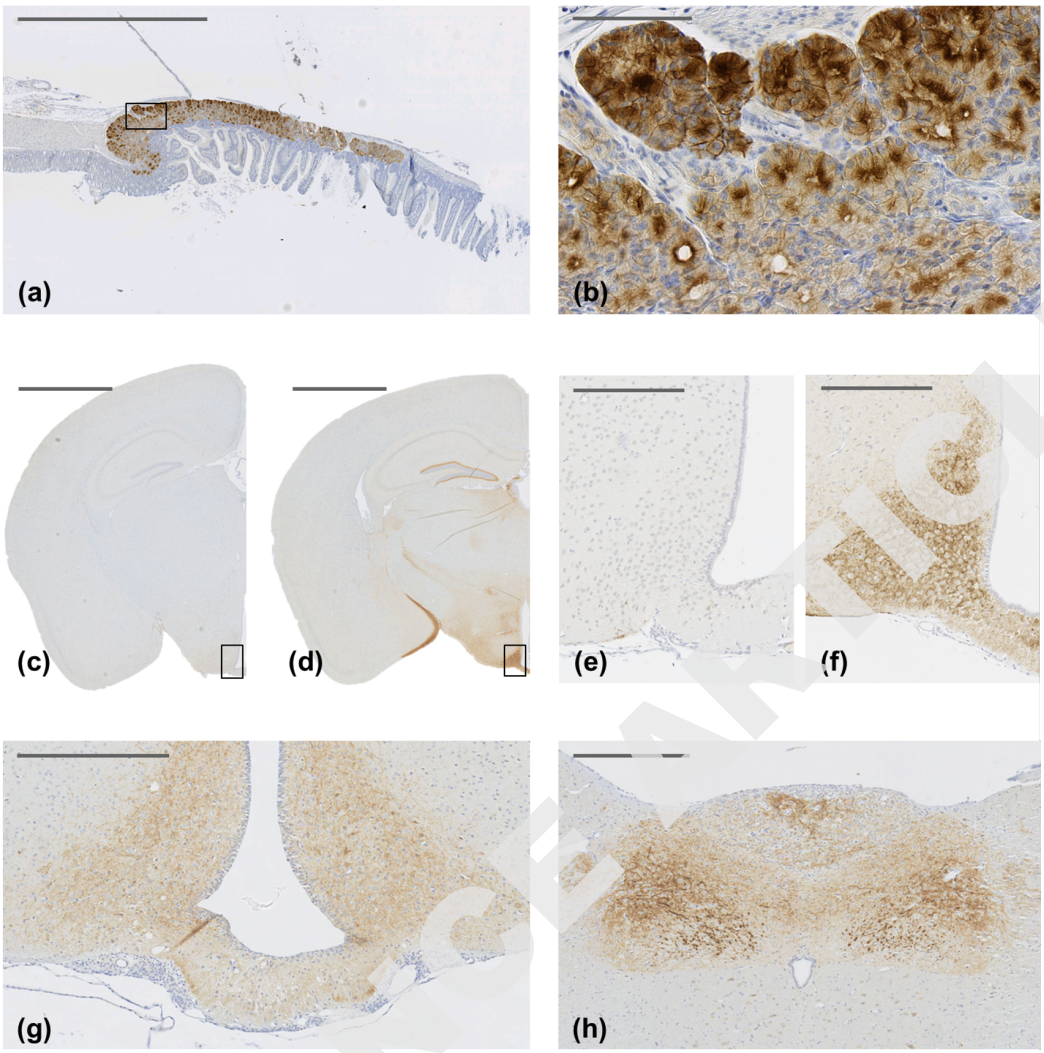

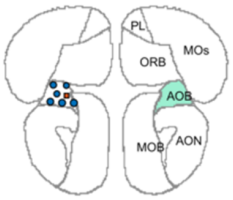

Bregma 2.86

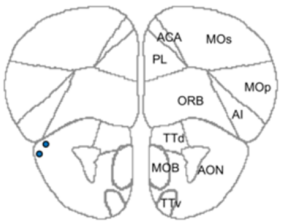

Bregma 2.34

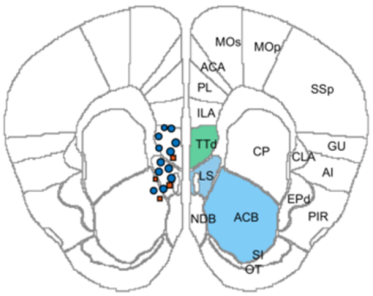

Bregma 1.70

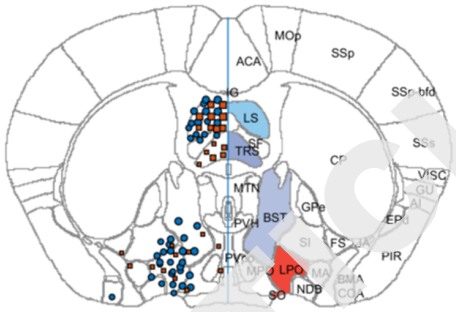

Bregma -0.22

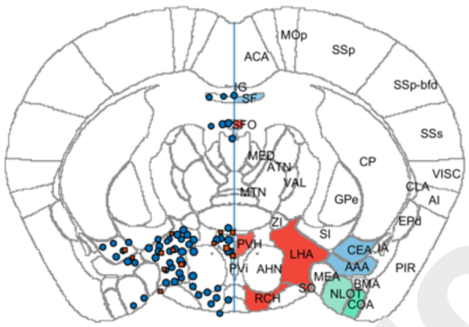

Bregma -0.70

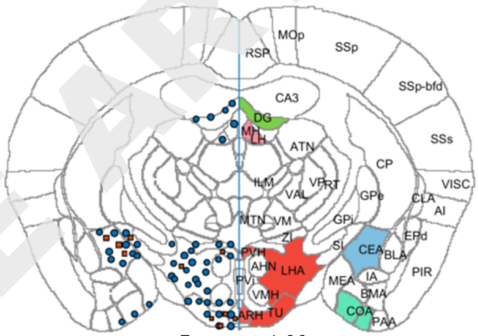

Bregma -1.06

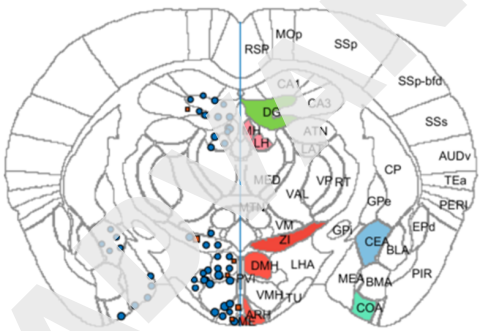

Bregma -1.46

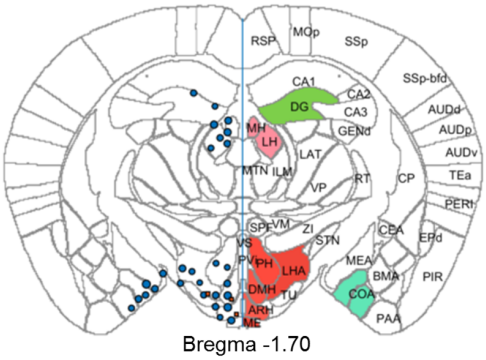

Bregma -1.70

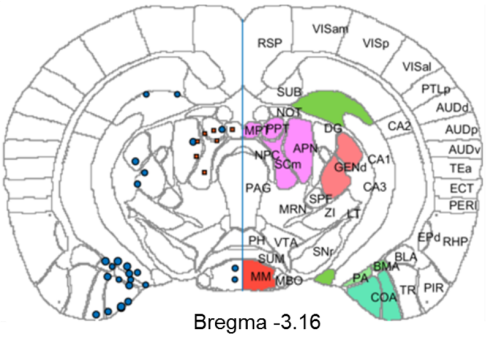

Bregma -3.16

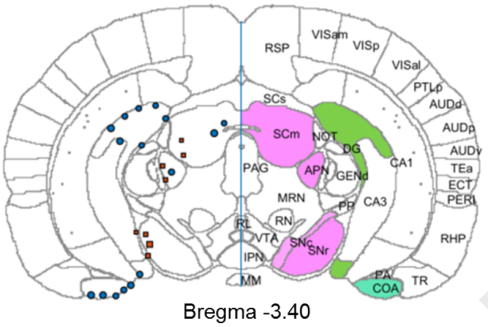

Bregma -3.40

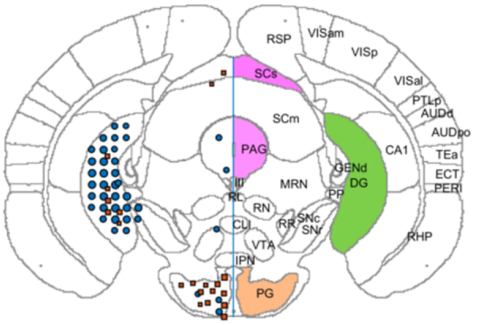

Bregma -4.16

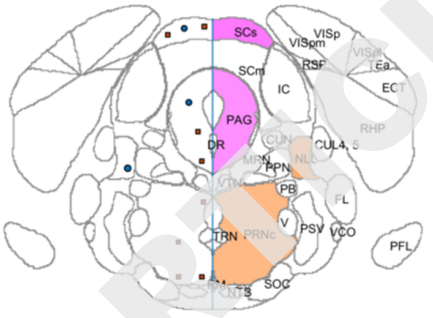

Bregma -4.84

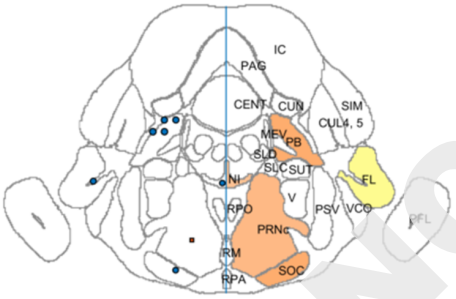

Bregma -5.20

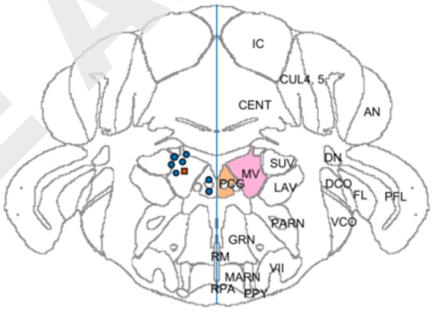

Bregma -5.80

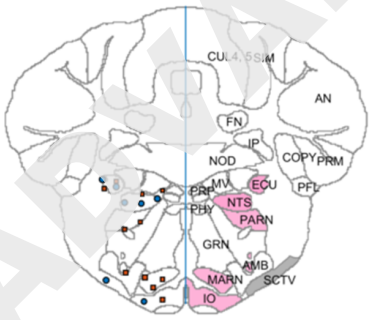

Bregma -6.72

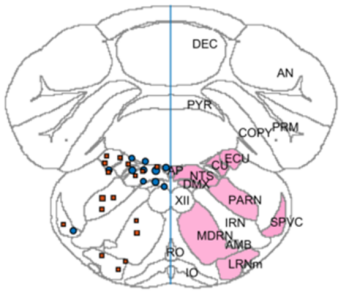

Bregma -7.32